JOURNAL OF MATERIALS SCIENCE 22 (1987) 1635–1641

Phase relations in the ternary system Cu–In–Se

U.-C. BOEHNKE, G. KÜHN
Karl-Marx-Universität Leipzig, Sektion Chemie, WB Kristallographie, 7010 Leipzig, GDR

The phase relations of the ternary system Cu–In–Se were studied at 750° C by quenching experiments. Special attention was given to the region $CuInSe_2$–In_2Se_3–In_4Se_3. Only four ternary phases with extended homogeneity ranges were found to exist. They were characterized by X-ray powder diffraction, electron microprobe analysis (EMPA), and optical microscopy. Differential thermal analysis (DTA) investigations allowed us to construct the T–x diagram of the Cu_2Se–In_2Se_3 cut between 47 and 100 mol % In_2Se_3. Besides, it was also possible to give a tentative diagram of the solid–liquid equilibria at 750° C and to get some information on the sub-solidus existence fields beside the Cu_2Se–In_2Se_3 cut.

1. Introduction

Although the thin film solar cell (Cd, Zn)S/$CuInSe_2$ is considered for commercial use [1] the current knowledge of the phase relations in the ternary system Cu–In–Se is rather incomplete. It seems that this system is the most complex of all A^I–B^{III}–C^{VI} systems so far investigated.

Till now the relevant papers have mainly been focused on the tie-line Cu_2Se–In_2Se_3 [2–13]. Numerous compounds were stated to exist along this line but there are evident differences concerning their structure, homogeneity range and thermal behaviour. Table I and Fig. 1 summarize the literature data. Besides, Konešova *et al.* [10] and Bachmann *et al.* [11, 12], also studied the solid–liquid relations in special regions beside the Cu_2Se–In_2Se_3 cut so that the liquidus surface can be considered as clarified. However, investigations of the sub-solidus field are rather rare.

In this paper we will report the phase relations of the region $CuInSe_2$–In_2Se_3–In_4Se_3 which is of most interest.

2. Experimental techniques

The samples were typically prepared by direct synthesis from a mixture of the elements in evacuated double-wall fused silica ampoules with a minimum of free volume. All starting materials used were 5N pure. According to our knowledge of the reaction mechanism the heating procedure had to be interrupted at about 280° C for one day [14]. The mechanical homogenization of the melt at 1100° C was followed by annealing for 20 days at 750° C and quenching down to room temperature. Estimations of the diffusion mean path length [15–17] show that for the experimental conditions chosen the equilibrium state could approximately be attained in the In-poorer region.

The resulting ingots were polycrystalline. The phase analysis and the determination of the lattice parameters were performed by X-ray powder diffraction using filtered CuKα radiation and silicon as the internal standard.

A special preparation had to be used for samples showing a layered structure. In order to prevent a preferential orientation in the sample holder the powder, made by rubbing with a diamond wheel, was additionally mixed with cork flour. The X-ray investigations at higher temperatures were carried out by means of a Guinier-Lenné camera for which the sample was placed in fused silica capillaries.

The chemical composition was determined by wavelength dispersive electron microprobe analysis, EMPA. Because of problems with the determination of the absolute values the measuring system was calibrated by sensitive wet analysis methods: coulometry for the copper- and the indium content and gravimetry for the selenium-content [18]. In this way an accuracy of about 4% could be reached. It should be mentioned at this point that Hwang *et al.* [19] observed the same problems with respect to the dependence of the detected values on the measuring conditions.

The thermal behaviour was studied by means of a Setaram microthermoanalyser in the temperature range from 500 to 1150° C ($\Delta T = \pm 5$ K) and of a Setaram DSC-111 apparatus in the temperature range from 25 to 770° C ($\Delta T = \pm 3$ K) at a heating rate of 3 K min^{-1}. The transformation temperatures were generally defined to be the onset temperature of the DTA peak.

3. Results and discussion

3.1. The Cu_2Se–In_2Se_3 cut

On quasibinary consideration of the Cu_2Se–In_2Se_3 cut the T–x diagram presented in Fig. 2 for the range between 47 and 100 mol % In_2Se_3 could be derived from our experiments. While the liquidus nearly corresponds to that of Konešova *et al.* [10] the established phase relations in the solid region are in contradiction to theirs. We found four ternary phases which will be now discussed.

At 750° C the homogeneous region of ordered $CuInSe_2$ with chalcopyrite structure (α-phase) extends from 47.5 to 55.0 mol % In_2Se_3. The deviation perpendicular to the cut estimated along the iso-Cu-lines is ±1 at % and lies within the error limits of EMPA. Therefore, only non-molecularity could be detected. The lattice parameters do not change distinctly within

0022-2461/87 $03.00 + .12

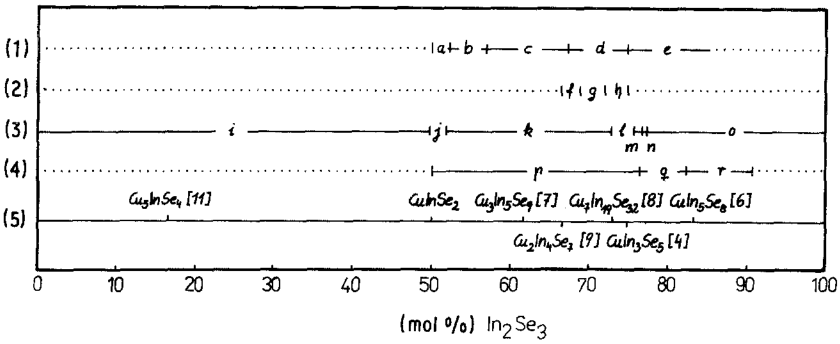

Figure 1 Literature survey of phases along the Cu_2Se–In_2Se_3 cut (see Table I). (1) Palatnik *et al.* [2], (2) Djega-Mariadassou *et al.* [8], (3) Konešova *et al.* [10] (room temperature), (4) Folmer *et al.* [13] (600° C $\leqslant T \leqslant$ 800° C), (5) stoichiometric compounds.

the whole homogeneous range (Table II). The cation/anion (c/a) ratio is constant and amounts to 2.009 ± 0.001. By means of high temperature X-ray investigations of stoichiometric $CuInSe_2$ only the transformation at 810° C into the disordered modification with sphalerite structure (δ-phase) was observed. An additional transformation at 665° C claimed to occur by Becker and Wagner [16] could not be detected. The δ-phase will be described later.

The β-phase extends from 66.5 to 79.0 mol % In_2Se_3 at 750° C. Within the considered triangle $CuInSe_2$–In_2Se_3–In_4Se_3 the deviation perpendicular to the Cu_2Se–In_2Se_3 cut is less than 1 at %. The X-ray powder diffractogram is quite similar to that of the α-phase, only with some additional weak reflections (Fig. 3) and therefore suggests a chalcopyrite-like ordered defect structure with a body-centred tetragonal lattice [9]. While the lattice parameters decrease slightly with increasing In_2Se_3-content the c/a ratio varies from 2.000 ± 0.001 to 2.003 ± 0.001 in the same direction (Table II). Besides, the characteristic additional reflections become stronger and consequently the conditions for such an ordered defect structure become more favourable. However, the ideal cation/anion ratio of the only possible structures (the thiogallate structure or the defect stannite structure), that is 3/4, will not be reached in our case.

The β-phase shows no phase transformations. Its In_2Se_3–richest composition starts to melt at about 880° C. At 930° C the β-phase of 66 mol % In_2Se_3 decomposes peritectically into the δ-phase (65 mol % In_2Se_3) and melt (80 mol % In_2Se_3). With respect to the literature, it can be concluded that the compounds $Cu_2In_4Se_7$ described by Schumann *et al.* [9] and $CuIn_5Se_8$ described by Manolikas *et al.* [6] as well as the pseudocubic phase given by Palatnik *et al.* [2, 20] for the region between 67.6 and 75.0 mol % In_2Se_3, the cubic $Cu_8In_{18}Se_{32}$ and the tetragonal $Cu_7In_{19}Se_{32}$ observed by Djega-Mariadassou *et al.* [8] all belong to the β-phase presented here. Moreover, the space group $P\bar{4}3m$ proposed by Lesueur *et al.* [21] and Djega-Mariadassou *et al.* [8] for their $Cu_8In_{18}Se_{32}$ conflicts with the indexing of the diffraction pattern since some special extinction rules can be derived.

The γ-phase extends between 82.0 and 90.0 mol % In_2Se_3 at 750° C. Within the considered triangle $CuInSe_2$–In_2Se_3–In_4Se_3 the deviation perpendicular to the Cu_2Se–In_2Se_3 cut is about 1.5 at %. The γ-phase has a typical layered structure which is easily perceptible with the naked eye (Fig. 4). The micrograph of this phase shows regions with different hardness and reflectance (see also Fig. 7). By X-ray powder analysis we found two modifications, a hexagonal (γ_H) and a trigonal (γ_T) one. They occur both alone and in coexistence in one ingot, but γ_T seems to be favoured on the In_2Se_3-poorer side of the homogeneous range. The

TABLE I Survey of the phases along the Cu_2Se–In_2Se_3 cut reported in the literature (Phase notation illustrated in Fig. 1.)

Notation	Observed phases	Remarks
a	one	chalcopyrite phase
b	mixed	metastable structures of decomposition
c	mixed	detection of two tetragonal phases
d	one	pseudocubic phase
e		complex layered structure
f	one	homogeneity range of cubic $Cu_8In_{18}Se_{32}$
g		intermediate region
h	one	homogeneity range of tetragonal $Cu_7In_{19}Se_{32}$
i	two	α-Cu_2Se and chalcopyrite phase
j	one	chalcopyrite phase
k	two	chalcopyrite phase and σ-phase (homogeneity range of $CuIn_3Se_5$)
l	one	σ-phase
m	two	σ-phase and sphalerite phase
n	one	sphalerite phase
o	two	sphalerite phase and α-In_2Se_3
p		cubic stacking region of close-packed Se layers and tetragonal ordering of Cu/In and metal/vacancy divided into the three one-phase regions: γ, γ', γ''
q	two	
r	mixed	mixed cubic/hexagonal stacking region of close-packed selenium layers with three polytypes: ε, ζ, η

TABLE II Lattice parameters as a function of the chemical composition for the ternary Cu–In–Se phases

Phase	Composition (at %)			Lattice parameters (determined at room temperature)		c/a-ratio
	Copper	Indium	Selenium	a(nm)	c(nm)	
α-phase	25.8	24.9	49.3	0.5785 ± 0.0001	1.1621 ± 0.0006	2.009 ± 0.001
	22.1	27.0	50.9	0.5780 ± 0.0001	1.1610 ± 0.0003	2.009 ± 0.001
β-phase	15.2	31.0	53.8	0.5766 ± 0.0001	1.1531 ± 0.0003	2.000 ± 0.001
	11.5	32.9	55.6	0.5751 ± 0.0001	1.1520 ± 0.0006	2.003 ± 0.001
γ-phase γ_T	7.3	35.0	57.7	1.212 ± 0.002	4.604 ± 0.001	
γ_T	7.0*	35.6	57.4	1.212 ± 0.002	4.604 ± 0.001	
γ_H				0.4040 ± 0.0008	3.271 ± 0.001	
γ_H	4.3	37.2	58.5	0.4040 ± 0.0002	3.272 ± 0.001	
δ-phase	24.4†	25.6	50.0	0.584 ± 0.002		
	14.0	32.3	53.7	0.5755 ± 0.0001		
	11.8	33.7	54.5	0.5746 ± 0.0001		

*γ_T and γ_H coexisted in one ingot.
†determined at 940° C.

TABLE III X-ray powder diffraction data of the two γ-modifications (observed d-spacings)

Hexagonal modification γ_H			Trigonal modification γ_T		
$d[10^{-10}\text{m}]$	hkl	I/I_0	$d[10^{-10}\text{m}]$	hkl	I/I_0
16.3	002	1	9.2	005	1
10.9	003	2	8.9	103	1
8.2	004	2	7.7	006	5
6.52	005	12	6.57	007	3
5.45	006	9	5.76	008	13
4.67	007	14	5.11	009	5
4.07	008	100	4.60	$00\underline{10}$	1
3.63	009	8	4.24	$10\underline{10}$	1
3.50	100	4	4.19	$00\underline{11}$	5
3.42	102	5	3.84	$00\underline{12}$	100
3.33	103	2	3.54	$00\underline{13}$	3
3.27	$00\underline{10}$	27	3.49	301	3
3.21	104	18	3.40	217	3
3.08	105	5	3.29	$00\underline{14}$	26
2.973	$00\underline{11}$	3	3.25	$11\underline{12}$	11
2.942	106	3	3.07	$00\underline{15}$	1
2.798	107	1	2.927	224	1
2.725	$00\underline{12}$	12	2.877	$00\underline{16}/21\underline{11}$	21
2.520	$00\underline{13}/109$	6	2.752	227	1
2.388	$10\underline{10}$	1	2.558	$00\underline{18}/404$	2
2.266	$10\underline{11}$	4	2.369	$10\underline{19}$	1
2.180	$00\underline{15}$	4	2.343	409	1
2.150	$10\underline{12}$	15	2.279	$40\underline{10}/412$	1
2.044	$00\underline{16}$	2	2.193	$00\underline{21}/416$	1
2.020	110	12	2.169	$40\underline{12}$	2
1.942	$10\underline{14}$	9	2.117	$20\underline{20}/31\underline{15}$	8
1.919	$00\underline{17}$	7	2.092	$00\underline{22}/419$	2
1.851	$10\underline{15}$	5	2.023	$22\underline{17}/330$	7
1.817	$00\underline{18}$	3	2.002	$00\underline{23}/41\underline{11}$	1
1.811	118	4	1.969	$41\underline{12}$	2
1.765	$10\underline{16}/119$	3	1.903	338	1
1.718	$00\underline{19}/11\underline{10}$	1	1.881	$41\underline{14}$	5
1.710	204	2	1.838	$00\underline{25}/41\underline{15}$	1
1.686	$10\underline{17}$	1	1.819	$33\underline{11}$	1
			1.791	$41\underline{16}/33\underline{12}$	2
			1.771	$00\underline{26}$	2
			1.759	$33\underline{13}/600$	2
			1.719	$33\underline{14}/51\underline{11}$	1
			1.654	$33\underline{16}$	1
			1.645	$00\underline{28}$	1

Chemical composition γ_H: 4.5 at % Cu; 36.2 at % In; 59.3 at % Se
γ_T: 7.3 at % Cu; 35.0 at % In; 57.7 at % Se

observed d-spacings of γ_H and γ_T together with their indexing are given in Table III. The data of the γ_T-phase are in very good agreement with those of Folmer *et al.* [13] for their ε-phase. Our γ_H-phase seems to be the equivalent of the η-phase of Folmer *et al.*, but there is only a correspondence in the (0 0 1) reflections. Their ζ-phase could not be observed. With respect to the lattice parameters determined (Table II) it is evident that:

(i) except for the occurrence of two different modifications there is no dependence of the lattice parameters on composition;

(ii) the two γ-modifications are polytypes like the two α-In_2Se_3 modifications and their structure can also be derived from the structure of the OD (order/disorder)-basis layer of In_2Se_3 calculated by Schauber *et al.* [22].

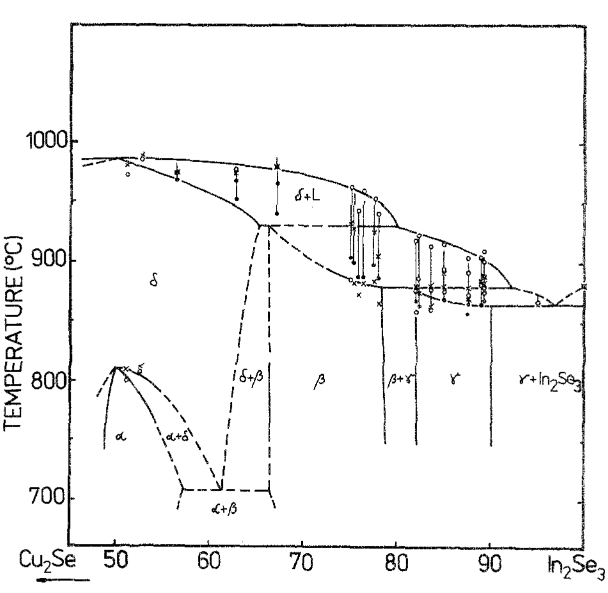

Figure 2 T–x diagram of the Cu_2Se–In_2Se_3 cut in the range $47 < x \leqslant 100$ mol % In_2Se_3. (The cut is considered to be a quasi-binary one.) Heating: (×) endothermic peak, (●) endothermic baseline intercept, (——) melting interval. Cooling: (○) exothermic peak.

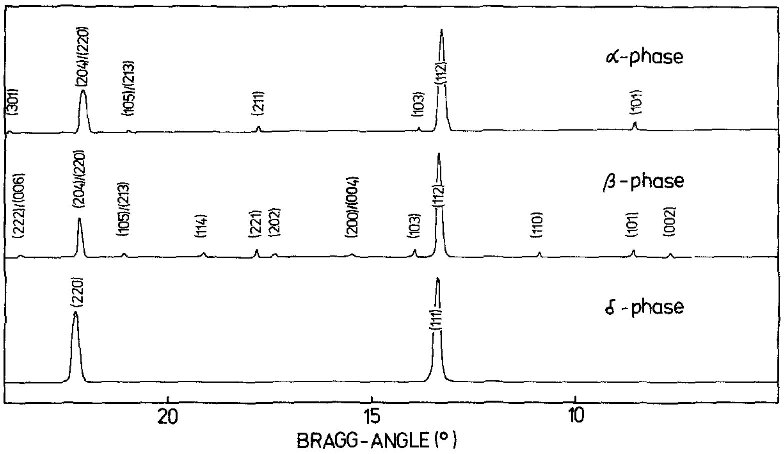

Figure 3 Schematic drawings of the X-ray powder patterns for the α-, β-, and δ-phase, (Ni-filtered Cu*K*α radiation.)

The a-axes of both γ-phases correspond exactly to those of α-In_2Se_3 [23], i.e.

$$a(\gamma_T) = 3a(\alpha\text{-}In_2Se_3) = \sqrt{3}a_{OD} \qquad (1)$$

and

$$a(\gamma_H) = a(\alpha\text{-}In_2Se_3) = \sqrt{3}/3a_{OD} \qquad (2)$$

On the other hand the c-axes increase slightly, i.e.

$$c(\gamma_T) = 14.3c_{OD} \qquad (3)$$

and

$$c(\gamma_H) = 10.2c_{OD} \qquad (4)$$

with $a_{OD} = 0.711$ nm and $c_{OD} = 0.321$ nm [22]. Therefore, the incorporation of copper influences only the c-direction. This might mean that copper does not occupy indium sites but tends to be a cation between the layers of In_2Se_3. The In_2Se_3-richest composition of the γ-phase starts to melt at 865° C. At about 880° C the γ-phase of 82 mol % In_2Se_3 decomposes peritectically into the β-phase (78 mol % In_2Se_3) and melt (92.5 mol % In_2Se_3). Sometimes we observed for γ_H an additional but very small DTA peak at about 750° C which may indicate a phase transformation to γ_T.

As mentioned above, the δ-phase represents the homogeneity region of the disordered modification of $CuInSe_2$. By high temperature X-ray powder investigations we could prove the transition from the chalcopyrite to the sphalerite structure. A determination of the phase boundaries of the δ-phase along the Cu_2Se–In_2Se_3 cut was not possible. But we found it to be stabilized down to room temperature beside this cut, in the range between 15.5 and 11.0 at % copper along the tie-line $CuInSe_2$–$In_{0.42}Se_{0.58}$. This region represents a copper deficiency with respect to the stoichiometric composition and a selenium deficiency with respect to the β-phase. Fig. 3 schematically shows the X-ray powder diffractogram of the δ-phase in comparison to those of the α- and the β-phase. In Table II the measured lattice parameters are listed. They decrease with decreasing copper-content as reported for the α- and β-phase. By DTA investigations we found an extensive melting interval over the whole range of δ-stabilization. The resulting liquidus (Fig. 5) matches that of the Cu_2Se–In_2Se_3 cut within the considered region quite well (cf. Fig. 2)).

The occurrence of the δ-phase down to room temperature quite near the Cu_2Se–In_2Se_3 cut led us to doubt that this cut is really quasibinary. The multiphase region situated between the one-phase regions of α, β and δ cannot be detected precisely. Firstly, as indicated in Fig. 3 the X-ray powder diffractograms of these three phases are quite similar. Besides, EMPA investigations failed in this case because of the very small compositional differences and last but not least because of the possibility of submicroscopic intergrowths especially as a consequence of the decomposition of the δ-phase as long as it is not stabilized.

The other two-phase fields along the Cu_2Se–In_2Se_3 cut are clarified. The α-phase is in equilibrium with Cu_2Se. Fig. 6 shows the micrograph of these two phases in a typical eutectic arrangement.

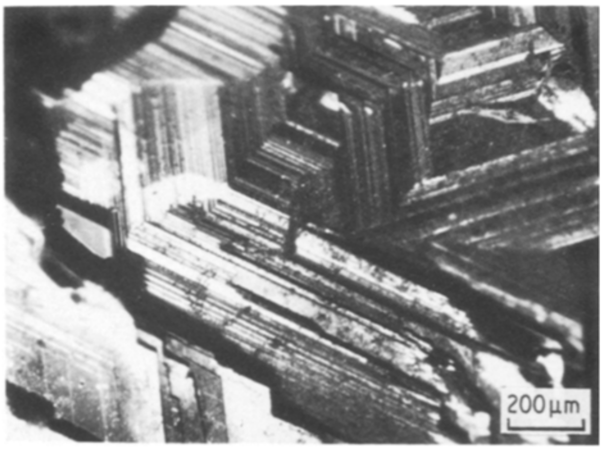

Figure 4 Photomicrograph of the γ-phase, surface of an ingot (The sample was crystallized from a melt of 90 mol % In_2Se_3.)

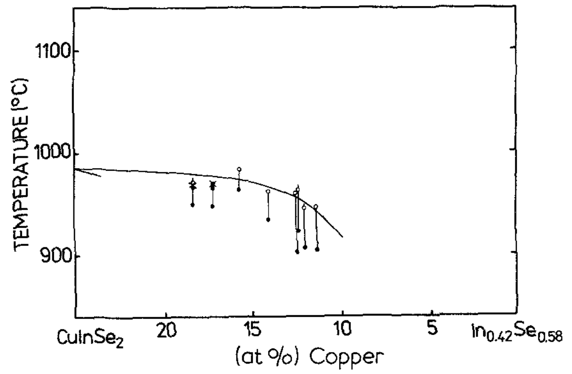

Figure 5 Tentative liquidus along the $CuInSe_2$–$In_{0.42}Se_{0.58}$ tie-line with $x \geq 11$ at % Cu. Heating: (×) endothermic peak, (●) endothermic baseline intercept, (——) melting interval. Cooling: (○) exothermic peak.

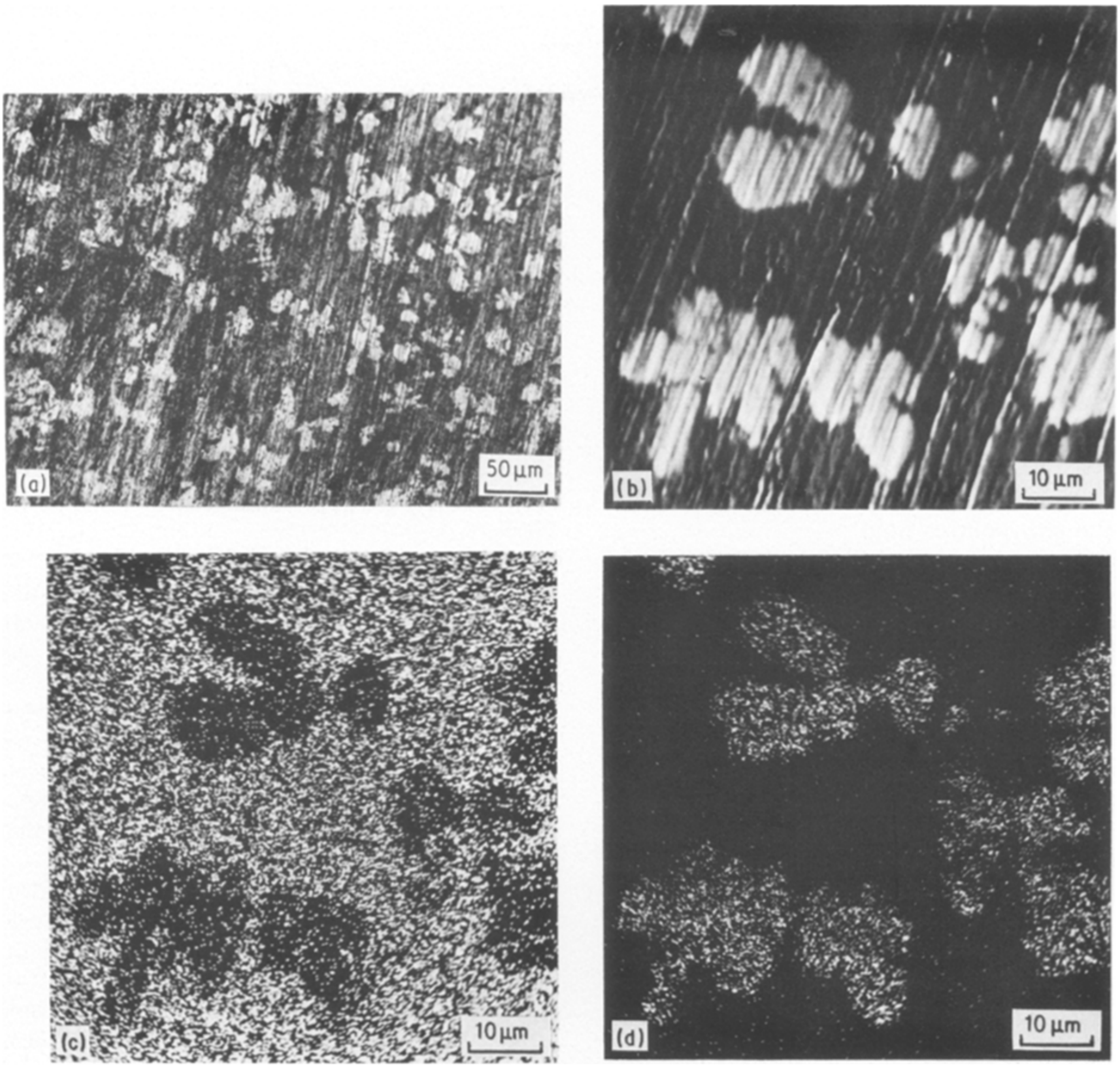

Figure 6 Dendrites of the α-phase surrounded by Cu_2Se (a) photomicrograph (b) scanning electron image, (c, d) X-ray scanning pictures of $CuK\alpha$ and $InL\alpha$ radiation, respectively. (The sample was crystallized from a melt of 10 mol % In_2Se_3).

From the DTA and microscopic investigations we did not get any hints on the existence of the additional (high temperature) compound Cu_5InSe_4 reported by Bachmann *et al.* [11, 12]. Due to the peritectic reaction the β- and the γ-phase occur only separately within their two-phase region (Fig. 7). On the other hand the γ-phase and In_2Se_3 form an eutectic microstructure. The structural analogies effect mostly lamellar intergrowth (Figs 8 and 9).

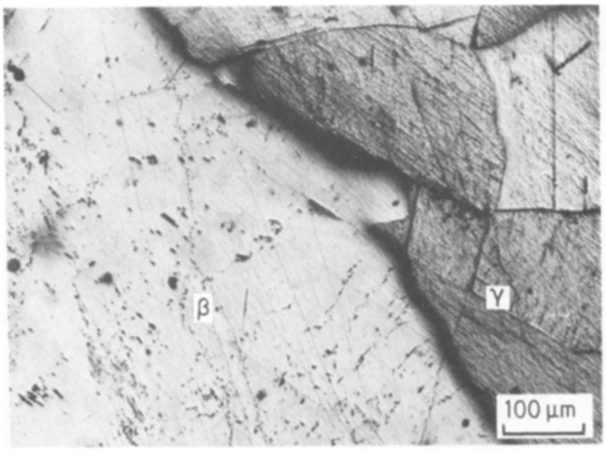

Figure 7 Photomicrograph of the phase boundary between the β- and the γ-phase. (The sample was crystallized from a melt of 80 mol % In_2Se_3.)

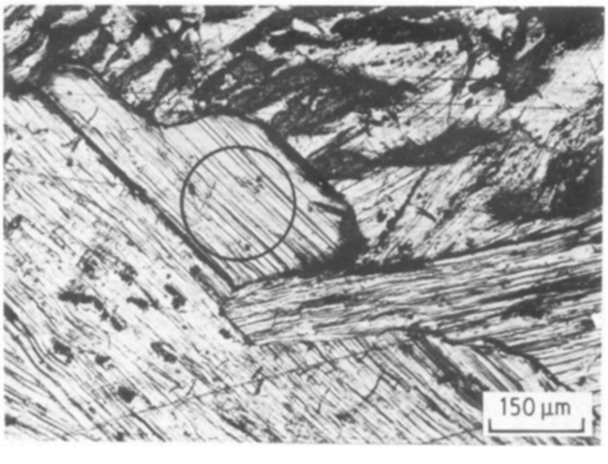

Figure 8 Photomicrograph of the fine- to coarse-crystalline lamellar intergrowths of the γ-phase and In_2Se_3. (The sample was crystallized from a melt of 95 mol % In_2Se_3.)

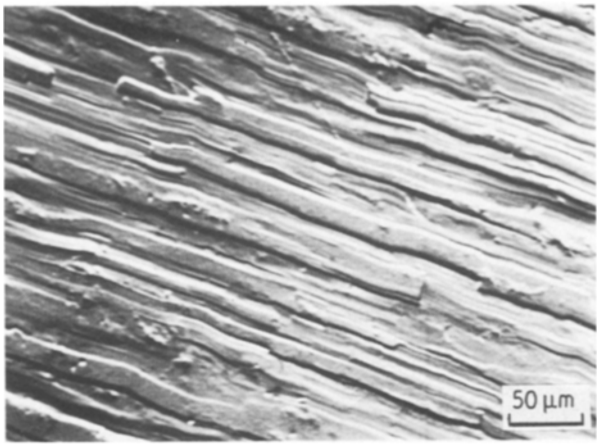

Figure 9 Scanning electron image of the marked part in Fig. 8.

3.2. The solid–liquid equilibria at 750° C and the sub-solidus field

On the basis of previous studies by Konešova *et al.* [10] and Bachmann *et al.* [12] and of our results we can give a tentative diagram of the solid–liquid equilibria at 750° C (Fig. 10). The only solid phases are Cu (ss), Cu_2Se (ss), In_2Se_3 and the α-, β-, γ-, and δ-phase.

Investigating the secondary crystallized part of the ingots we obtained some information on the sub-solidus existence fields besides the Cu_2Se–In_2Se_3 cut. Though the extensive ranges of liquid immiscibility also cause non-equilibrium phases to crystallize the following phase equilibria can be assumed:

$$\alpha\text{-phase} + CuSe$$

$$\alpha\text{-phase} + In_4Se_3 + InSe$$

$$\alpha\text{-phase} + In_4Se_3 + Cu_{11}In_9$$

$$\delta\text{-phase} + InSe + In_6Se_7$$

$$\gamma\text{-phase} + In_6Se_7 + In_2Se_3$$

Besides, the equilibrium between the α-phase and selenium has already been described by Konešova *et al.* [10].

The β-phase forms no equilibria with any compound of the Se-poorer region of the system. it is masked by the δ-phase. The phases α and δ prefer a dendritic growth in coexistence with other binary compounds.

4. Conclusions

The phase relations of the ternary system Cu–In–Se were studied at 750° C by quenching experiments. Special interest was given to the region $CuInSe_2$–In_2Se_3–In_4Se_3. As reported earlier for the Cu–Ga–Se system [24] and the Cu–Ga–S system [25], we found in the Cu–In–Se system the formation of ternary compounds to be restricted to the $A^{I}_2C^{VI}$–$B^{III}_2C^{VI}_3$ cut and its vicinity. Four ternary phases, the α-, β-, γ-, and δ-phase, could be detected. Their homogeneous ranges were estimated.

The α-phase represents the ordered $CuInSe_2$ modification with chalcopyrite structure. Its transformation into the disordered modification with sphalerite structure (δ-phase) could be experimentally verified for the first time by high temperature X-ray powder diffraction.

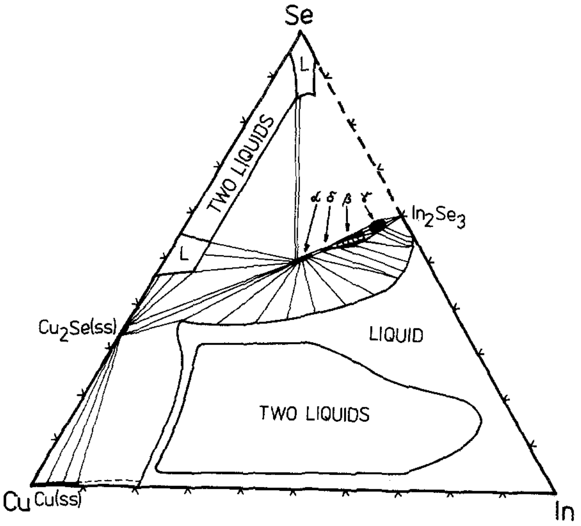

Figure 10 Ternary solid-liquid relations in the Cu–In–Se system at 750° C.

While the δ-phase occurs only as a high temperature phase along the Cu_2Se–In_2Se_3 cut it is stabilized down to room temperature on the metal-rich side near this cut.

The β-phase crystallizes in an ordered chalcopyrite-like defect structure. From a comparison of its X-ray powder data with those of the literature for ternary compounds such as $Cu_2In_4Se_7$, $Cu_8In_{18}Se_{32}$, $Cu_7In_{19}Se_{32}$, $CuIn_3Se_5$, and $CuIn_5Se_8$ it is evident that all these compounds belong to the β-phase.

The γ-phase has a typical layered structure. It occurs in two modifications, a hexagonal and a trigonal one. These modifications are polytypes like the two α-In_2Se_3 modifications.

The T–x diagram of the Cu_2Se–In_2Se_3 cut here presented for the range between 47 and 100 mol % In_2Se_3 gives a new interpretation of the sub-liquidus field.

Similar to the Cu–Ga–Se system [24] the liquid immiscibility behaviour is dominated beside this cut especially in the metal-rich region. Therefore difficulties encountered during the growth of $CuGaSe_2$ and $CuInSe_2$ from a Ga- or In-rich melt are not surprising.

Acknowledgements

The authors would like to thank S. Rolle for assistance with microprobe measurements at the Technische Universität Dresden. They are also indebted to Dr B. Schumann and Dr P. Schreiter for valuable discussions.

References

1. R. A. MICKELSEN, in Proceedings of the Polycrystalline Thin Film Review Meeting, Golden (Colorado), May 1983 (Solar Energy Research Institute Publication CP 211-1985).
2. L. S. PALATNIK, JU. F. KOMNIK and Ė. I. ROGAČĖVA, *Ukr. Fiz. Ž.* **9** (1964) 862.
3. L. S. PALATNIK and Ė. I. ROGAČĖVA, *Dokl. AN SSSR* **174** (1967) 80.
4. D. M. GANBAROV, G. G. GUSEJNOV and Z. Š. KARAEV, *Izv. AN SSSR, Neorg. Mater.* **8** (1972) 2211.
5. J. PARKES, R. D. TOMLINSON, and M. J. HAMPSHIRE, *J. Cryst. Growth* **20** (1973) 315.
6. C. MANOLIKAS, J. v. LANDUYT, R. de RIDDER, and S. AMELINCKX, *Phys. Status Solidi* (*a*) **55** (1979) 709.
7. V. T. TAGIROV, N. F. GACHRAMANOV, A. G.

GUSEJNOV and F. M. ALIEV, *Kristallografija* **25** (1980) 411.

8. C. DJEGA-MARIADASSOU, A. RIMSKY, R. LESUEUR and H. J. ALBANY, in Proceedings of the 4th International Conference on Ternary and Multinary Compounds, Tokyo, 1980, *Jpn J. Appl. Phys., Suppl.* **19(3)** (1980) 89.
9. B. SCHUMANN, G. KÜHN, U. BOEHNKE, and H. NEELS, *Kristallografija* **26** (1981) 1195.
10. T. I. KONEŠOVA, A. A. BABICYNA, and V. T. KALINNIKOV, *Izv. AN SSSR, Neorg. Mater.* **18** (1982) 1483.
11. M. FEARHEILEY and K. J. BACHMANN, in Proceedings of the Symposium on Materials and New Processing Technologies for Photovoltaics, Princeton, 1983 (ECS Publication 8311, 1983) p. 469.
12. K. J. BACHMANN, M. FEARHEILEY, Y. H. SHING and N. TRAN, *Appl. Phys. Lett.* **44** (1984) 407.
13. J. C. W. FOLMER, J. A. TURNER, R. NOUFI and D. CAHEN, *J. Electrochem. Soc.* **132** (1985) 1319.
14. G. KÜHN and U. BOEHNKE, *J. Cryst. Growth* **61** (1983) 415.
15. S. WAGNER, in Proceedings of the Electrochemical Society Meeting, San Francisco, May 1983, p. 410.
16. K. D. BECKER and S. WAGNER, *Phys. Rev.* **B27** (1983) 5240.
17. H. J. v. BARDELEBEN, *J. Appl. Phys.* **56** (1984) 321.
18. A. KÖHLER, thesis (Diplomarbeit), Karl-Marx-Universität Leipzig (1983).
19. H. L. HWANG, C. M. FOU, S. SHEA, V. DALTON, M. H. YANG and C. S. SHEN, in Proceedings of the 6th International Conference on Ternary and Multinary Compounds, Caracas, August 1984, *Prog. Cryst. Growth Charact.* **10** (1984) 175.
20. L. S. PALATNIK and Ë. I. ROGAČËVA, *Izv. AN SSSR, Neorg. Mater.* **2** (1966) 478.
21. R. LESUEUR, C. DJEGA-MARIADASSOU, P. CHARPIN and H. J. ALBANY, in Proceedings of the Third International Conference on Ternary Compounds, Edinburgh, 1977, *Inst. Phys. Conf. Ser.* **35** (1977) 15.
22. H. SCHRAUBER, H. GRELL, K.-O, BACKHAUS and K. FICHTNER, private communication.
23. S. POPOVIĆ, A. TONEJC, B. GRŽETA-PLENKOVIĆ, B. ČELUSTKA and R. TROJKO, *J. Appl. Cryst.* **12** (1979) 416.
24. J. C. MIKKELSEN Jr, *J. Electronic Mater.* **10** (1981) 541.
25. M. KOKTA, J. R. CARRUTHERS, M. GRASSO, H. M. KASPER and B. TELL, *ibid.* **5** (1976) 69.

Received 2 June
and accepted 18 August 1986